

Perpendicular magnetic anisotropy in a Pt/Co/Pt ultrathin film arising from a lattice distortion induced by ion irradiation

M. Sakamaki and K. Amemiya

*Photon Factory and Condensed Matter Research Center, Institute of Materials Structure Science,
High Energy Accelerator Research Organization, Tsukuba, Ibaraki 305-0801, Japan*

M. O. Liedke and J. Fassbender

Helmholtz-Zentrum Dresden-Rossendorf, 01328 Dresden, Germany

P. Mazalski, I. Sveklo, and A. Maziewski

Department of Physics, University of Białystok, ul. Lipowa 41, Białystok, Poland

(Received 15 April 2012; published 16 July 2012)

Ga^+ irradiation-induced changes in magnetic anisotropy and crystalline structure of a Pt/Co/Pt ultrathin film are investigated by means of x-ray magnetic circular dichroism (XMCD) and extended x-ray absorption fine structure (EXAFS) techniques. The XMCD analysis shows a large orbital moment difference between out-of-plane and in-plane directions, which corresponds to perpendicular magnetic anisotropy (PMA), at moderate Ga^+ fluences, while further increased fluences reduce the orbital moment difference resulting in in-plane magnetization. From the EXAFS analysis, enhancement of PMA is directly related to an in-plane lattice expansion caused by ion irradiation and Co-Pt intermixing, which results in a large lattice distortion. Thus, the origin of the ion irradiation-induced changes in magnetic anisotropy is successfully explained.

DOI: [10.1103/PhysRevB.86.024418](https://doi.org/10.1103/PhysRevB.86.024418)

PACS number(s): 75.30.Gw, 61.80.Jh, 78.70.Dm

I. INTRODUCTION

A lot of efforts have been made to realize perpendicular magnetic anisotropy (PMA) in thin films and multilayers, especially in view of the application to high-density magnetic recording media. Among them, the control of magnetic anisotropy by ion irradiation has attracted much interest in this decade,^{1–8} due to a possibility of nanostructure patterning by using a focused ion beam.^{3,5} In fact, a Ga^+ -induced spin reorientation transition to perpendicular magnetization from in-plane magnetized Pt/Co/Pt thin films has recently been reported both at medium^{1,2} and high² ion fluences, which are in 10^{14} and 10^{15} ions/cm² regions, respectively.

As possible changes induced by ion irradiation, Co-Pt intermixing and an $L1_0$ -type ordered alloy formation have been suggested. Vieu *et al.* proposed ion-induced collisional intermixing at the Co-Pt interface,⁵ which has been confirmed by transmission electron microscopy (TEM).² Maziewski *et al.* showed that the Co K -edge x-ray magnetic circular dichroism (XMCD) spectrum of the Ga^+ -irradiated Pt/Co/Pt film is similar to that of the $L1_0$ -type ordered alloy.² On the other hand, R. Hyndman *et al.* indicated, by means of TEM, that Pt grain size and texture in a Co/Pt multilayer increase by Ga^+ irradiation.⁴ A structural study by using XRD and extended x-ray absorption fine structure (EXAFS) reveals that relaxation of tensile strain in Co layer reduces PMA.⁹ However, the origin of the ion-induced appearance of PMA has not been understood from the structural point of view, though the lattice distortion must play an essential role in the determination of magnetic anisotropy.

In this paper, we unambiguously show, by means of Co K -edge EXAFS, that the in-plane lattice constant of the Co film is significantly expanded by a medium Ga^+ irradiation of 1.5×10^{14} ions/cm², while the out-of-plane one is relatively

unaffected. This results in a large distortion in the Co film structure, which would induce PMA. Upon a higher Ga^+ fluence of 4×10^{14} ions/cm², the out-of-plane lattice constant is also expanded, and the Co film structure becomes almost isotropic, which coincides with the disappearance of PMA. Moreover, an angle-dependent XMCD analysis at the Co L edge shows that the Ga^+ irradiation-induced changes in the orbital moment anisotropy of Co are consistent with observed magnetic anisotropy of the Pt/Co/Pt film, and with the magnetoelastic anisotropy energy estimated from the EXAFS results.

II. EXPERIMENTAL

A 2.4 nm Co film sandwiched by 4.5 nm Pt underlayer and 3.5 nm Pt overlayer was prepared on a (0001) sapphire substrate by sputter deposition. The film was then irradiated as contiguous 1-mm-wide regions with Ga^+ ion fluences increasing from 0 to 7×10^{14} ions/cm².

The Co $L_{\text{III,II}}$ -edge XMCD spectra were taken at the soft x-ray undulator beamline, BL-16A, of the Photon Factory in the Institute of Materials Structure Science, High Energy Accelerator Research Organization (KEK-PF). All the XMCD spectra were recorded at room temperature in the total-electron-yield mode, in which the drain current from the sample was measured. The XMCD measurements were performed both in an applied magnetic field of 1.2 T and in the remanent state after magnetizing the sample with a magnetic field pulse of ~ 0.05 T. The applied magnetic fields were parallel and antiparallel to the x-ray propagation direction. We adopted the normal and grazing incidence configurations for the XMCD measurements, in which the angle between the surface normal and the x-ray beam, θ , was 0° and 55° or 60° ,

respectively, in order to examine magnetic anisotropy of the film.

The Co *K*-edge EXAFS spectra were measured at the bending magnet beamline BL-12C of KEK-PF. All the spectra were recorded at 20 K in the fluorescence-yield mode with a 19-element solid-state detector. To examine crystallographic anisotropy in the Co thin film, the EXAFS spectra were taken at normal and grazing incidence configurations at $\theta = 0^\circ$ and 60° , respectively.

III. RESULT AND DISCUSSION

A. XMCD

XMCD spectra taken in the remanent magnetization state are shown in Fig. 1(a). Since the XMCD intensity is basically proportional to the magnetization component parallel to the x-ray beam, a larger XMCD intensity at $\theta = 0^\circ$ than that at $\theta = 60^\circ$ directly shows the appearance of PMA, which is the case at Ga^+ ion fluences of $1 - 2 \times 10^{14}$ ions/cm². On the other hand, the XMCD intensity is significantly larger at $\theta = 60^\circ$ both at no irradiation and higher fluences above $\sim 3 \times 10^{14}$ ions/cm². These changes in magnetic anisotropy are consistent with the reported behavior of the Ga^+ -irradiated Pt/Co/Pt films.^{1,2}

Then we measured XMCD spectra under an applied magnetic field of 1.2 T, as shown in Fig. 1(b), in order to estimate the magnetic anisotropy energy of the Co film. All the data exhibit almost the same intensities between two different incidence angles. This indicates that the magnetic saturation is achieved in both the normal and the in-plane directions of the film at 1.2 T, which allows us to directly determine anisotropy of the orbital magnetic moment. We estimate the spin magnetic moment, m_s , and the in-plane and out-of-plane orbital magnetic moments, m_l^\parallel and m_l^\perp , respectively, from the analysis of the angle dependence in the XMCD data.^{10,11} According to the angle-dependent XMCD theory, m_s is directly obtained by applying the spin sum rule^{12,13} to the XMCD data at $\theta = 55^\circ$, which is called the magic angle. On the other hand, m_l^\parallel and m_l^\perp are separately determined by using the XMCD data taken at different incidence angles according to the following

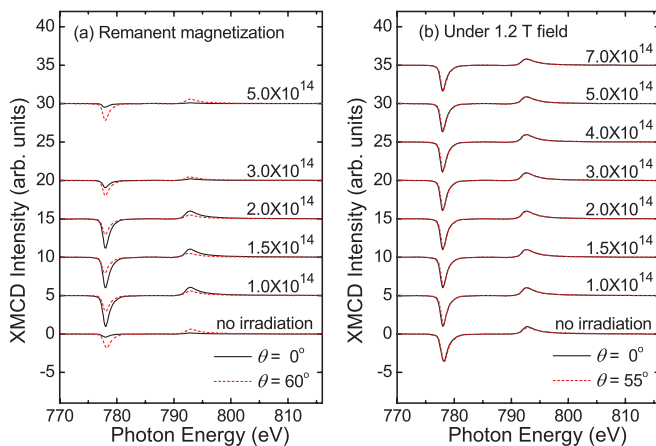


FIG. 1. (Color online) Co *L*-edge XMCD spectra for a Pt/Co/Pt film with indicated Ga^+ ion fluences taken with remanent magnetization (a) and under a 1.2 T field (b) at the normal (solid line) and grazing (dashed line) incidence angles.

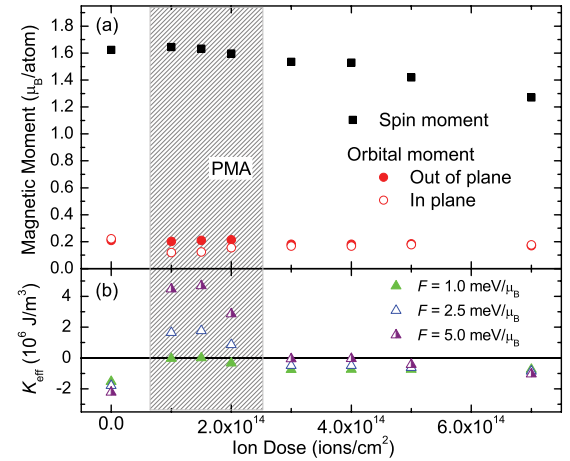


FIG. 2. (Color online) Spin (square) and out-of-plane (filled circle) and in-plane (open circle) orbital magnetic moments of Co in a Pt/Co/Pt film estimated at 1.2 T as functions of Ga^+ ion fluence, obtained from the incidence-angle dependence of the XMCD spectra (a), together with magnetic anisotropy energy, K_{eff} , including shape anisotropy, estimated from the orbital moments by assuming indicated proportionality factors, F (b). A shaded area corresponds to the appearance of PMA.

relation;

$$m_l^\theta = m_l^\parallel \sin^2 \theta + m_l^\perp \cos^2 \theta, \quad (1)$$

where m_l^θ denotes the orbital magnetic moment obtained by applying the orbital sum rule¹² to the XMCD spectrum taken at an incidence angle θ . The estimated m_s , m_l^\parallel , and m_l^\perp are indicated in Fig. 2(a).

For the nonirradiated Co film, in which in-plane magnetization is obtained at remanence, m_l^\parallel is slightly larger than or almost the same as m_l^\perp . On the other hand, m_l^\perp is significantly larger than m_l^\parallel at Ga^+ fluence of $1 - 2 \times 10^{14}$ ions/cm², in which PMA is observed. At higher Ga^+ fluences, corresponding to in-plane magnetization again, the difference between m_l^\parallel and m_l^\perp almost disappears. The effective magnetic anisotropy energy K_{eff} of a film is related to the difference between m_l^\parallel and m_l^\perp as expressed by

$$K_{\text{eff}} = -2\pi M^2 + F(m_l^\perp - m_l^\parallel), \quad (2)$$

where M and F are the saturation magnetization and a proportionality factor, respectively.^{14,15} By adopting this simple relation, we can estimate K_{eff} for the Co film. Since various F values have been reported ranging from 0.7 to 50 meV/ μ_B ,^{15,16} we plot the estimated K_{eff} for $F = 1, 2,$ and 5 meV/ μ_B in Fig. 2(b). Magnetic anisotropy of the present film is well reproduced by assuming $F \sim 1-5$ meV/ μ_B . Although this estimation seems reasonable considering the recent report, in which $F = 2.0$ and 3.0 meV/ μ_B are obtained for Fe and Ni, respectively,¹⁶ we do not quantitatively determine the magnetic anisotropy energy here but focus on the tendency of the orbital moment anisotropy of Co. From this point of view, the Ga^+ irradiation-induced changes in magnetic anisotropy are interpreted by those in anisotropy of the Co orbital moment.

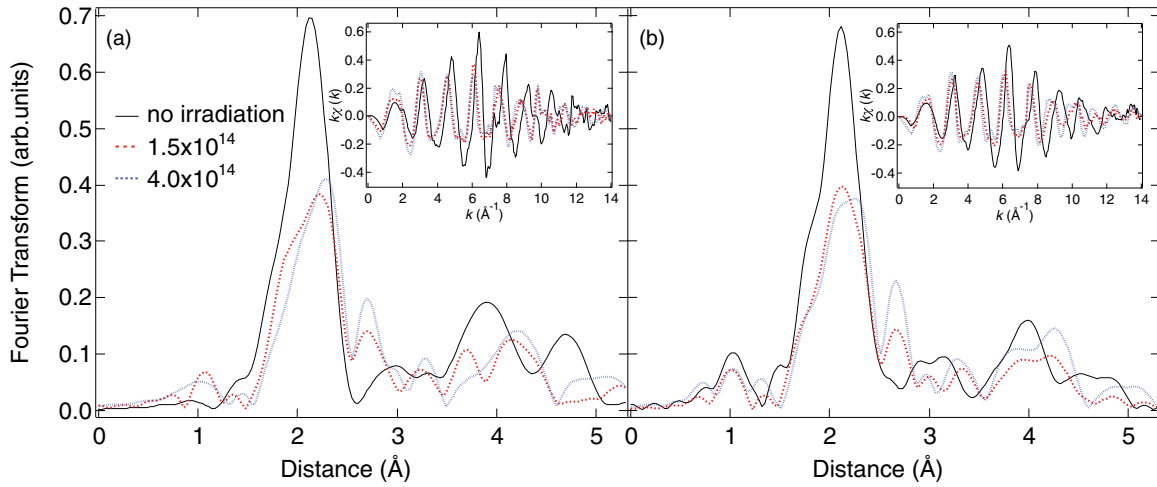


FIG. 3. (Color online) Fourier transforms of the Co *K*-edge EXAFS function, $k\chi(k)$ (inset), of a Pt/Co/Pt film with different Ga^+ ion fluences, 0 (solid line), 1.5×10^{14} (dashed line), and 4.0×10^{14} ions/cm² (dotted line), taken at the normal (a) and grazing (b) incidence angles.

B. EXAFS

Figure 3 shows Fourier transforms of the Co *K*-edge EXAFS function $k\chi(k)$ of a Pt/Co/Pt film with different Ga^+ ion fluences. For the nonirradiated Co film, a sharp peak at a distance of $\sim 2 \text{ \AA}$, which corresponds to the nearest Co-Co bond, is observed. Note that the phase shift effect in EXAFS is not corrected, so that the peak appears at a shorter distance than the actual one. With increasing Ga^+ fluence, the amplitude of the peak rapidly decreases and the peak shifts towards the larger distance, suggesting a reduction of the coordination number and an expansion of the Co-Co bond length. Moreover, another peak appears at $\sim 2.5 \text{ \AA}$, which grows with increasing Ga^+ fluences, directly indicating the contribution from the Co-Pt bond due to the intermixing between Co and Pt. These changes are also recognized in the $k\chi(k)$ spectra in Fig. 3.

We further analyze the EXAFS data in order to obtain quantitative structural parameters. EXAFS curve fittings are performed by IFEFFIT package^{17,18} in *k* space after the inverse Fourier transform for the nearest Co-Co and Co-Pt

contributions. The EXAFS spectra for the L1₀-type ordered structure¹⁹ calculated by FEFF8 code²⁰ are used as a theoretical standard. In-plane and out-of-plane bond lengths are separately determined by simultaneous fitting of the EXAFS data taken both at 0° and 60°. Experimental and fitted Co *K*-edge EXAFS functions with different Ga^+ ion fluences taken at the grazing incidence angle are shown in Fig. 4, while the obtained structural parameters are given in Table I.

For the nonirradiated film, the EXAFS data are well fitted by taking only the Co-Co bond into account, due to little Co-Pt intermixing. The Co-Co bond lengths are almost isotropic and similar to that of bulk hcp Co. In contrast, at a Ga^+ irradiation of 1.5×10^{14} ions/cm², the in-plane lattice constant is significantly expanded by 4.8%, while the out-of-plane bond length shows a relatively small expansion of 2.4%. This structural change might be because Co atoms are struck out by Ga^+ irradiation and/or intermixing with Pt occurs in the vicinity of the Co/Pt interface. In fact, a large coordination number for the Co-Pt bond is obtained for the irradiated film, suggesting significant Co-Pt intermixing. Such a large lattice

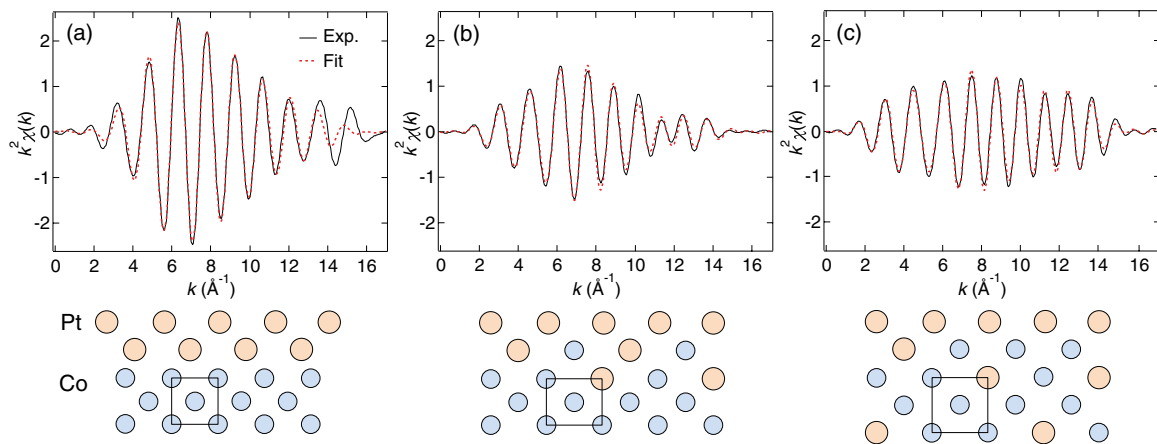


FIG. 4. (Color online) Comparison between the experimental (Exp.) and fitted (Fit) Co *K*-edge EXAFS functions, $k^2\chi(k)$, for a Pt/Co/Pt film with different Ga^+ ion fluences, 0 (a), 1.5×10^{14} (b), and 4.0×10^{14} ions/cm² (c) taken at the grazing incidence angle. Schematic illustrations of the obtained structural parameters are also given.

TABLE I. Structural parameters for a Pt/Co/Pt film with indicated Ga⁺ ion fluences (ions/cm²) obtained by fitting the Co *K*-edge EXAFS data after the inverse Fourier transform for the nearest Co-Co and Co-Pt contributions. r , N , and σ^2 represent bond length, coordination number, and Debye-Waller factor, respectively. We assume that the energy shift of the absorption edge, ΔE_0 , of Co-Co shell is equivalent to that of Co-Pt shell.

Ion fluence (ions/cm ²)		Co-Co bond			Co-Pt bond			ΔE_0 (eV)
		r (Å)	N	σ^2 (Å ²)	r (Å)	N	σ^2 (Å ²)	
0.0	In-plane	2.504(4)	3.5(4)	0.0041(8)				0.0(7)
	Out-of-plane	2.505(5)	3.6(5)	0.0052(9)				
1.5×10^{14}	In-plane	2.625(18)	1.5(8)	0.0058(37)	2.684(21)	3.5(1.5)	0.0089(27)	0.2(1.0)
	Out-of-plane	2.564(10)	2.1(5)	0.0069(19)	2.661(8)	1.3(6)	0.0033(18)	
4.0×10^{14}	In-plane	2.642(15)	1.3(6)	0.0045(32)	2.683(11)	2.9(9)	0.0057(16)	0.6(6)
	Out-of-plane	2.630(13)	1.8(6)	0.0097(32)	2.667(4)	2.2(5)	0.0033(8)	

distortion would enhance PMA through the magnetoelastic effect in the Co film.^{21,22} If we assume the magnetoelastic constants of bulk Co,²² the obtained lattice distortion results in an increase in the magnetoelastic anisotropy energy by 2.0×10^6 J/m³. This increase explains the appearance of PMA in the present sample because this value can overcome the shape anisotropy energy, $-2\pi M^2 = -1.2 \times 10^6$ J at a Ga⁺ irradiation of 1.5×10^{14} ions/cm².

At a higher Ga⁺ fluence of 4×10^{14} ions/cm², the out-of-plane Co-Co bond length expands by 5.0% compared with that for the nonirradiated sample, which is now almost the same as the in-plane bond. Such an isotropic structure would lose PMA. In fact, from a similar estimation of the magnetoelastic anisotropy energy one yields a decrease of 0.8×10^6 J/m³ compared to that estimated at a Ga⁺ irradiation of 1.5×10^{14} ions/cm². In addition, the coordination number of out-of-plane Co-Co decreases, while that of out-of-plane Co-Pt increases, indicating that Co-Pt intermixing increases and more Pt atoms exist in the Co layers.

IV. SUMMARY

In summary, we have shown, by means of Co *K*-edge EXAFS, that the in-plane lattice constant of the Pt-sandwiched Co film is significantly expanded by 4.8% at a medium Ga⁺ irradiation of 1.5×10^{14} ions/cm², while the out-of-plane one is relatively unaffected (+2.4%). This results in a large

distortion in the Co film structure, which induces PMA through the magnetoelastic effect. At a higher Ga⁺ fluence of 4×10^{14} ions/cm², the out-of-plane lattice constant is also expanded to +5.0%, and the Co film structure becomes almost isotropic, which coincides with the disappearance of PMA. The Co-Pt intermixing is also confirmed by EXAFS, though it is not capable of determining the L1₀-type ordered structure. Moreover, an angle-dependent XMCD analysis at the Co *L* edge has shown that the Ga⁺ irradiation-induced changes in orbital moment anisotropy of Co are essentially consistent with observed magnetic anisotropy of the Pt/Co/Pt film, and with the magnetoelastic anisotropy energy estimated from the EXAFS results. Thus, the origin of irradiation-induced magnetic anisotropy is successfully explained by a combination of the XMCD and EXAFS techniques.

ACKNOWLEDGMENTS

The present work has been performed under the approval of the Photon Factory Program Advisory Committee (Proposal Nos. 2010S2-001 and 2011G552). The authors are grateful for the financial support of the Quantum Beam Technology Program from the Ministry of Education, Culture, Sports, Science and Technology (MEXT), Japan, and SYMPHONY project operated within the Foundation for Polish Science Team Programme co-financed by the EU European Regional Development Fund, OPIE2007–2013.

¹J. Jaworowicz, A. Maziewski, P. Mazalski, M. Kisielewski, I. Sveklo, M. Tekielak, V. Zablotskii, J. Ferré, N. Vernier, A. Mougin, A. Henschke, and J. Fassbender, *Appl. Phys. Lett.* **95**, 022502 (2009).

²A. Maziewski, P. Mazalski, Z. Kurant, M. O. Liedke, J. McCord, J. Fassbender, J. Ferré, A. Mougin, A. Wawro, L. T. Baczewski, A. Rogalev, F. Wilhelm, and T. Gemming, *Phys. Rev. B* **85**, 054427 (2012).

³J. Jaworowicz, V. Zablotskii, J.-P. Jamet, J. Ferré, N. Vernier, J.-Y. Chauleau, M. Kisielewski, I. Sveklo, A. Maziewski, J. Gierak, and E. Bourhis, *J. Appl. Phys.* **109**, 093919 (2011).

⁴R. Hyndman, P. Warin, J. Gierak, J. Ferré, J. N. Chapman, J. P. Jamet, V. Mathet, and C. Chappert, *J. Appl. Phys.* **90**, 3843 (2001).

⁵C. Vieu, J. Gierak, H. Launois, T. Aign, P. Meyer, J.-P. Jamet, J. Ferré, C. Chappert, T. Devolder, V. Mathet, and H. Bernas, *J. Appl. Phys.* **91**, 3103 (2002).

⁶C. T. Rettner, S. Anders, J. E. E. Baglin, T. Thomson, and B. D. Terris, *Appl. Phys. Lett.* **80**, 279 (2002).

⁷N. Bergéard, J.-P. Jamet, J. Ferré, A. Mougin, and J. Fassbender, *J. Appl. Phys.* **108**, 103915 (2010).

⁸D. Stanescu, D. Ravelosona, V. Mathet, C. Chappert, Y. Samson, C. Beigné, N. Vernier, J. Ferré, J. Gierak, E. Bouhris, and E. E. Fullerton, *J. Appl. Phys.* **103**, 07B529 (2008).

⁹T. Devolder, S. Pizzini, J. Vogel, H. Bernas, C. Chappert, V. Mathet, and M. Borowski, *Eur. Phys. J. B* **22**, 193 (2001).

¹⁰J. Stöhr and H. König, *Phys. Rev. Lett.* **75**, 3748 (1995).

- ¹¹T. Koide, H. Miyauchi, J. Okamoto, T. Shidara, A. Fujimori, H. Fukutani, K. Amemiya, H. Takeshita, S. Yuasa, T. Katayama, and Y. Suzuki, *Phys. Rev. Lett.* **87**, 257201 (2001).
- ¹²B. T. Thole, P. Carra, F. Sette, and G. van der Laan, *Phys. Rev. Lett.* **68**, 1943 (1992).
- ¹³P. Carra, B. T. Thole, M. Altarelli, and X. Wang, *Phys. Rev. Lett.* **70**, 694 (1993).
- ¹⁴P. Bruno, *Phys. Rev. B* **39**, R865 (1989).
- ¹⁵J. Stöhr, *J. Magn. Magn. Mater.* **200**, 470 (1999).
- ¹⁶H. Abe, K. Amemiya, D. Matsumura, S. Kitagawa, H. Watanabe, T. Yokoyama, and T. Ohta, *J. Magn. Magn. Mater.* **302**, 86 (2006).
- ¹⁷M. Newville, *J. Synchrotron Radiat.* **8**, 322 (2001).
- ¹⁸B. Ravel and M. Newville, *J. Synchrotron Radiat.* **12**, 537 (2005).
- ¹⁹P. Villars and L. D. Calvert, *Pearson's Handbook of Crystallographic Data for Intermetallic Phase* (ASM, Meta Park, OH, 2000).
- ²⁰A. L. Ankudinov, C. E. Bouldin, J. J. Rehr, J. Sims, and H. Hung, *Phys. Rev. B* **65**, 104107 (2002).
- ²¹H. Fritzsche, J. Kohlhepp, and U. Gradmann, *Phys. Rev. B* **51**, 15933 (1995).
- ²²P. Bruno, *J. Phys. F* **18**, 1291 (1988).